AGU PUBLICATIONS

Geophysical Research Letters

RESEARCH LETTER
10.1002/2014GL062556

Key Points:
- In situ detection of cirrus in the extratropical stratosphere
- Focus on irreversible transport and small-scale mixing at the tropopause
- Cirrus particles affect the water vapor budget of the lowermost stratosphere

Supporting Information:
- Readme
- Figures S1 and S2

Correspondence to:
S. Müller,
Stefan.Mueller@uni-mainz.de

Citation:
Müller, S., P. Hoor, F. Berkes, H. Bozem, M. Klingebiel, P. Reutter, H. G. J. Smit, M. Wendisch, P. Spichtinger, and S. Borrmann (2015), In situ detection of stratosphere-troposphere exchange of cirrus particles in the midlatitudes, *Geophys. Res. Lett.*, *42*, 949–955, doi:10.1002/2014GL062556.

Received 18 NOV 2014
Accepted 18 JAN 2015
Accepted article online 24 JAN 2015
Published online 13 FEB 2015

In situ detection of stratosphere-troposphere exchange of cirrus particles in the midlatitudes

S. Müller[1], P. Hoor[1], F. Berkes[1], H. Bozem[1], M. Klingebiel[1], P. Reutter[1], H. G. J. Smit[2], M. Wendisch[3], P. Spichtinger[1], and S. Borrmann[1,4]

[1]Institute for Atmospheric Physics, Johannes Gutenberg University of Mainz, Mainz, Germany, [2]Institute for Energy and Climate Research, Research Centre Juelich GmbH, Juelich, Germany, [3]Leipzig Institute for Meteorology, University of Leipzig, Leipzig, Germany, [4]Max Planck Institute for Chemistry, Mainz, Germany

Abstract Airborne trace gas, microphysical, and radiation measurements were performed during the AIRcraft TOwed Sensor Shuttle - Inhomogeneous Cirrus Experiment over northern Germany in 2013. Based on high-precision nitrous oxide (N_2O) and carbon monoxide (CO) in situ data, stratospheric air could be identified, which contained cirrus cloud particles. Consistent with the stratospheric N_2O data, backward trajectories indicate that the sampled air masses crossed the dynamical tropopause in the last 3 h before the measurement. These air masses contained cirrus particles, which were formed during slow ascent in the troposphere and subsequently mixed with stratospheric air. From the CO-N_2O correlation the irreversibility of this transport is deduced. To our knowledge, this is the first in situ detection of cirrus particles mixed with stratospheric air in the midlatitudes.

1. Introduction

Riese et al. [2012] highlight the importance of understanding mixing processes in the upper troposphere/lower stratosphere (UTLS) to quantify the radiation budget of the atmosphere, especially in terms of water vapor and ozone. In this regard, we report on irreversible transport of cirrus cloud particles in stratospheric air using highly precise and fast airborne in situ N_2O measurements in the extratropical tropopause region (ExTL) [*Gettelman et al.*, 2011]. *Borrmann et al.* [1996] emphasized the potential impact of cirrus clouds on the abundance of ozone by heterogeneous chemical reactions on the particle surfaces. *Solomon et al.* [1997] suggested that cirrus clouds in the tropopause region may contribute to the observed depletion of ozone in the midlatitude lower stratosphere. Beside chemical aspects, the link between cirrus and the tropopause is still not clear. It gained increasing attention in the last decade with the discovery of the tropopause inversion layer (TIL) [see *Birner et al.*, 2002]. The TIL is characterized by a strong static stability peak of $N^2 = \frac{g}{\Theta}\frac{d\Theta}{dz}$ (g is the force of gravity, Θ is the potential temperature, and z is the altitude) right above the thermal tropopause. The mechanism of the formation and maintaining of the TIL are not yet fully understood. Besides large-scale dynamics [*Birner*, 2006] and baroclinic wave breaking [*Wirth*, 2003], *Randel et al.* [2007] suggest that radiative effects of both water vapor and ozone may have an important role in maintaining the TIL. Later, *Fusina et al.* [2007] investigated the radiative forcing of thin cirrus clouds. They concluded that their radiative impact strongly depends on the ice content and the size of the ice crystals.

It is obvious from the discussion above that the exact location of a cirrus cloud relative to the local tropopause affects their impact on the chemistry and radiation field in the UTLS. Therefore, a clear identification of the tropopause is essential. Currently several tropopause definitions are used in the literature, depending on the respective scientific question. The thermal tropopause has been defined as the level at which the (negative) temperature lapse rate decreases to 2 K km^{-1} or less and remains on average below 2 K km^{-1} for this level and any level within the next 2 km [*World Meteorological Organization (WMO)*, 1957]. Note that the static stability N^2 is directly linked to the dynamical definition of the tropopause [*Gettelman et al.*, 2011]. The dynamical tropopause is defined using a fixed potential vorticity (PV) [*Hoskins et al.*, 1985] ranging from 1 to 4 potential vorticity unit (pvu) (1 pvu = 10^{-6} K m^2 kg^{-1} s^{-1}) [*Randel et al.*, 2007]. *Kunz et al.* [2011] used the isentropic PV gradient to define the dynamical tropopause height from 1.5 to 5 pvu depending on season and latitude. Chemical substances (and their relations to each other) like ozone have been applied as a tropopause marker as well [*Zahn et al.*, 2000; *Fischer et al.*, 2000; *Hoor et al.*, 2002; *Pan*, 2004]. The latter definition refers to the so-called ozonopause which is either defined by an ozone

gradient [*Bethan et al.*, 1996] or threshold ozone mixing ratio between 60 and 200 ppbv [*Logan*, 1999], which has a strong seasonal cycle and regional variations as well.

In contrast to ozone, N_2O is chemically inert in the troposphere with a tropospheric lifetime of about 120 years [*Stratospheric Processes and their Role in Climate*, 2013], which leads to an almost homogeneous distribution in the troposphere. In July 2013, the tropospheric background N_2O mixing ratio was 326.4 ppbv (www.esrl.noaa.gov/gmd/hats/combined/N2O.html) with a seasonal cycle of $\pm$ 0.5 ppbv [*Jiang et al.*, 2007] and continuously increasing with a rate of 0.5–0.8 ppbv/yr [*Kort et al.*, 2011]. Importantly, the sinks of N_2O are entirely in the upper stratosphere, where it is mainly destroyed by the photolysis and reaction with $O(^1D)$. This chemical characteristic leads to a weak negative stratospheric N_2O gradient at the tropopause and makes it an appropriate tracer for the tropopause, since N_2O shows (in contrast to O_3) almost no variability or seasonality at the tropopause. Based on canister samples of N_2O collected during the Civil Aircraft for Regular Investigation of the Atmosphere Based on an Instrumented Container project, *Assonov et al.* [2013] determined a chemical tropopause for a climatological data set of 5 years. We apply this approach for high-resolution N_2O data which enabled the first in situ detection of cirrus particles in stratospheric air in the midlatitudes. There is some evidence of cirrus clouds in the midlatitude stratosphere on the basis of ground-based, reanalysis, or satellite data [*Keckhut et al.*, 2005; *Montoux et al.*, 2010; *Spang et al.*, 2014], but in situ identification cannot be found in the literature yet. Nevertheless, a frequent occurrence of ice supersaturation above the thermal tropopause, which is a prerequisite for persistent cirrus clouds in the stratosphere, was found by *Spichtinger et al.* [2003a, 2003b] from the analysis of radiosonde and satellite data.

2. The University of Mainz Airborne Quantum Cascade Laser-Spectrometer

The University of Mainz Airborne Quantum Cascade Laser-spectrometer (UMAQS) is based on an Aerodyne Quantum Cascade Laser Mini Monitor (Aerodyne Research Inc., MA, USA) with a 76 m astigmatic multipass absorption cell [*McManus et al.*, 2010, 2011] for simultaneous measurements of N_2O and CO mixing ratios. The instrument is based on direct absorption spectroscopy using a continuous-wave quantum cascade laser with a sweep rate of 2 kHz. At the end of each sweep the laser current is set below the threshold to determine the zero light level at the detector for the absorption measurement. During the flights a pressure controller keeps the measurement cell at a constant value typically at 70 mbar. To account for potential drifts, an in-flight calibration unit with compressed ambient air, which has been calibrated before and after the flights against a laboratory standard, was developed. The laboratory standard itself was measured externally against a NOAA standard with an uncertainty of $\pm$ 0.5 ppbv for N_2O and $\pm$ 1 ppbv for CO. A polynomial fit to the measured "Voigt-profile" centered at wave number $k = 2202.745\ cm^{-1}$ using the spectroscopical data from the HITRAN database calculates the trace gas mixing ratio of N_2O and CO. During the AIRTOSS-ICE campaign a time resolution of 1 Hz was reached, which is limited by the time for gas exchange of the measurement cell. For N_2O we achieved a precision of 0.16 ppbv (2σ) and an accuracy of 0.36 ppbv relative to the secondary standard. The simultaneously measured CO data from UMAQS at wave number $k = 2203.161\ cm^{-1}$ had a precision of 0.68 ppbv (2σ) and an accuracy of 1.22 ppbv. This leads to a total uncertainty (relative to the secondary standard) of N_2O = 0.39 ppbv and CO = 1.40 ppbv, respectively.

3. Detection of the N_2O-Based Chemical Tropopause During AIRTOSS-ICE 2013

UMAQS was deployed on a Learjet 35-A operated by the Gesellschaft für Flugzieldarstellung mbH/enviscope GmbH during the AIRTOSS-ICE (AIRcraft TOwed Sensor Shuttle - Inhomogeneous Cirrus Experiment) campaign over northern Germany in 2013. The campaign was designed to investigate the properties of cirrus clouds in the tropopause region with in situ trace gas, cloud particle, and radiation measurements. During May and August/September 2013, 12 flights over a restricted area centered at 54°N/7.2°E over the North Sea were performed. Additionally to the onboard instruments a towed sensor shuttle was attached to the aircraft to collect meteorological, radiation, and cloud particle data on a second level beneath the aircraft [*Frey et al.*, 2009]. During AIRTOSS - ICE 2013 the sensor shuttle was released from the wing of the aircraft by a steel rope with a length of approximately 900 m. At an airspeed of approximately 165 m/s, the shuttle is 180 m beneath and more than 800 m behind the aircraft. This paper reports on N_2O measurements from five flights in May and two flights in August 2013.

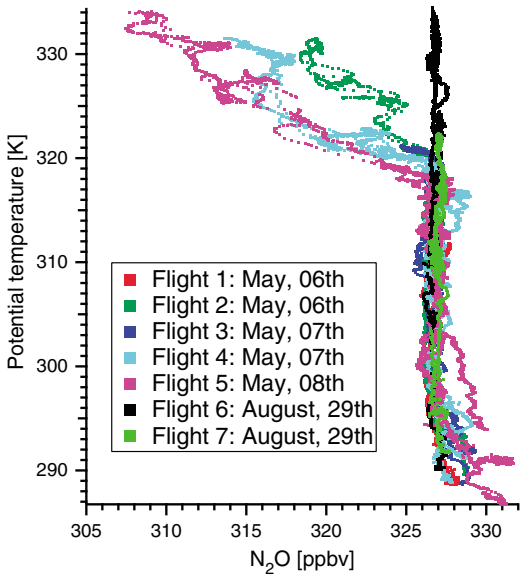

Figure 1. N_2O data as a function of potential temperature Θ (1 Hz data) from AIRTOSS-ICE 2013.

Figure 1 shows N_2O from seven flights (1 Hz data) as a function of potential temperature Θ. Between Θ = 290–315 K low variability of N_2O mixing ratios is evident, which indicates an almost homogeneous distribution of N_2O in the troposphere. The slight N_2O enhancement at lower levels, most obvious in flight 5, is related to recent precipitation stimulating N_2O emissions from soil. Importantly no values lower than N_2O = 325.5 ppbv are found below Θ = 315 K, which corresponds to the troposphere.

The abrupt change of the vertical N_2O gradient in the N_2O profiles around Θ = 320 K clearly indicates the N_2O-based chemical tropopause at this altitude. In contrast, fairly constant values of $N_2O > 325.5$ ppbv and the missing sharp gradient during flight 1 in May and flight 6 and 7 in August indicate that these flights did not reach the stratosphere. To quantify the tropospheric N_2O variability, all data points between 3 and 7 km for the flights in May (which corresponds to Θ = 290–310 K) and all data points of August were used (see Figure 1). Figure 2 shows the corresponding frequency distribution of these N_2O measurements in the free troposphere grouped by bins of 0.05 ppbv, without any further filtering.

N_2O in Figure 2 shows a mean and median of 326.8 ppbv and varies between 325.5 and 327.9 ppbv. This range is larger than the latitudinal variability of N_2O on the northern hemisphere of ± 0.5 ppbv [*Kort et al.*, 2011] and particularly exceeds the N_2O measurement uncertainty of UMAQS of 0.39 ppbv. The combination of both values leads to an upper limit for the uncertainty of the tropospheric N_2O mixing ratio during AIRTOSS-ICE of 0.9 ppbv.

Consequently, N_2O mixing ratios below the tropospheric range of 326.8 ± 0.9 ppbv clearly indicate air masses influenced by stratospheric air. N_2O mixing ratios above 327.7 ppbv are an indication for transport from the boundary layer (with the sources of N_2O) into the free troposphere.

The tropospheric N_2O value of 326.4 in July 2013 (www.esrl.noaa.gov/gmd/hats/combined/N2O.html) agrees with the measured tropospheric N_2O mixing ratio during AIRTOSS-ICE of 326.8 ± 0.9 ppbv. The small deviation of the mean value from AIRTOSS-ICE to the NOAA value can be explained either by the natural variability of N_2O [*Kort et al.*, 2011] or the uncertainty of the secondary standard of ± 0.5 ppbv. Importantly, this does not affect the calculation of the stratospheric threshold, because only the relative values of N_2O are crucial for the analysis in the following sections.

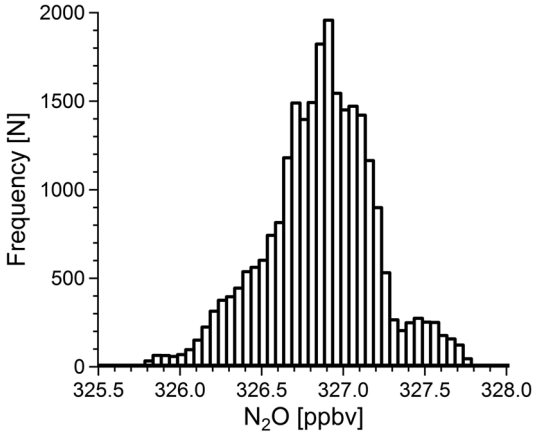

Figure 2. Frequency distribution of all available N_2O data in May and August between 3 km and 7 km during AIRTOSS-ICE 2013.

4. Cirrus Cloud Particles in a Stratospheric Surrounding

Figure 3 shows the vertical profiles of N_2O and CO between 9 and 11 km above sea level from AIRTOSS-ICE Flight 4 (8 May 2013) and the correlation of both species for the entire flight. Data points with simultaneously measured cirrus cloud particles at temperatures between −56 and −59°C by the Forward Scattering Spectrometer Probe (FSSP) instrument [*Dye and Baumgardner*, 1984; *Wendisch and Brenguier*, 2013] are marked red in Figures 3a and 3b. The size distribution of these particles (small box in Figure 3b) shows

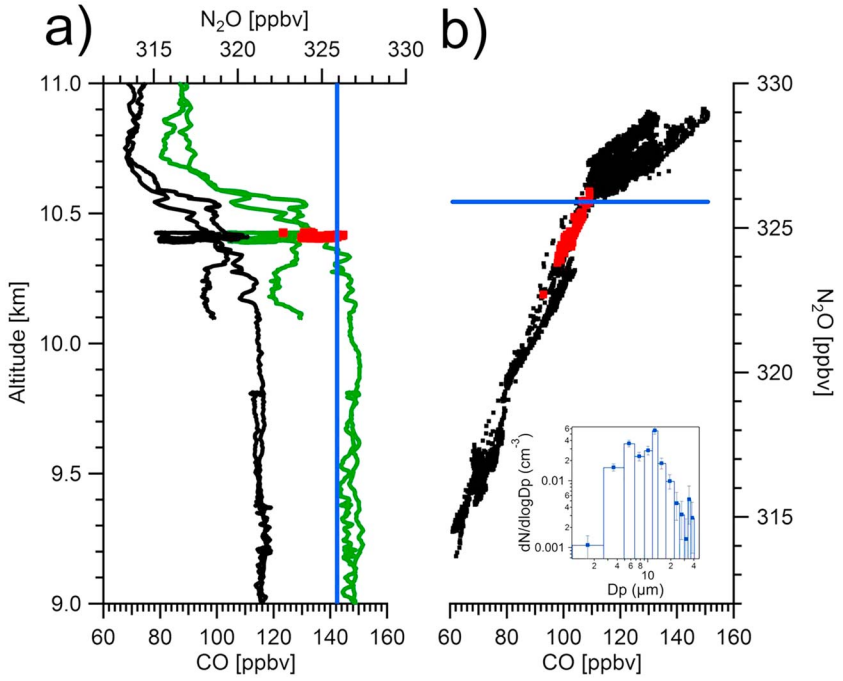

Figure 3. N_2O and CO data for AIRTOSS-ICE Flight 4 on 7 May 2013. (a) Vertical profile of N_2O (green) and CO (black) as a function of altitude in the range between 9 and 11 km. (b) CO-N_2O correlation of all data points from AIRTOSS-ICE Flight 4. Red dots mark data points with simultaneously measured cirrus cloud particles by the FSSP instrument in the tropopause region. Additionally the ice crystal size distribution is shown. In Figures 3a and 3b blue lines mark the N_2O threshold of 325.9 ppbv.

typical sizes and number concentrations of ice crystals in subvisual cirrus clouds [*Frey et al.*, 2011; *de Reus et al.*, 2009]. Importantly, the particles were detected in an air mass with ice supersaturation in the order of 10% (not shown). Satellite images (supporting information) show the propagation of a large cirrus cloud deck from the south into the flight area. From the fact that the shuttle 180 m below the aircraft is in cirrus clouds for almost the whole time period, the occurrence of the measured particles due to a former contrail is very unlikely. This is also indicated by the absence of a CO_2 peak [*Fahey et al.*, 1995] during the respective flight legs measured with the Fast Aircraft-Borne Licor Experiment (FABLE) Instrument [*Gurk et al.*, 2008].

However, as evident from Figure 3a, the cirrus particles are found in a region with N_2O values ranging from 322 to 326 ppbv, which are mainly well below the threshold of 325.9 ppbv and, therefore, in an air mass with stratospheric contribution in the tropopause region. The determination of the thermal tropopause from in situ temperature data for this flight section is not possible since the aircraft flew horizontally, and thus, no temperature profile is available. In situ temperature data during ascent and descent of the aircraft reveal the thermal tropopause at 10.1 and 10.4 km, respectively. This indicates a strong spatial and temporal variability of the thermal tropopause height in the measurement region. Additional radio soundings (supporting information) on 7 May 2013, 12 UTC and 8 May 2013, 00 UTC launched at Ekofisk (56.53°N, 3.21°E), Schleswig (54.53°N, 9.55°E), and Norderney (53.71°N, 7.15°E) confirm the finding of thermal tropopause heights between 10 and 11 km in the vicinity of the flight area.

The CO-N_2O scatterplot in Figure 3b shows two parts. A steep, almost linear slope with decreasing N_2O and CO values indicates stratospheric data. The tropospheric part is indicated by large variability of CO and a weak or missing correlation to CO accompanied with high N_2O. The transition between both parts is at $N_2O \approx 326$ ppbv. Notably, the stratospheric part of the correlation indicates irreversible mixing corresponding to the interpretation of the CO-O_3 correlation [*Hoor et al.*, 2002; *Pan*, 2004], since CO has negligible sources in the stratosphere. Importantly, the air masses with the measured ice crystals form a compact mixing line extending from the tropospheric to the stratospheric region in the CO-N_2O scatterplot. They are encountered above the mixing barrier which marks the tropopause, as evident from the change of the gradient of the CO-N_2O scatterplot.

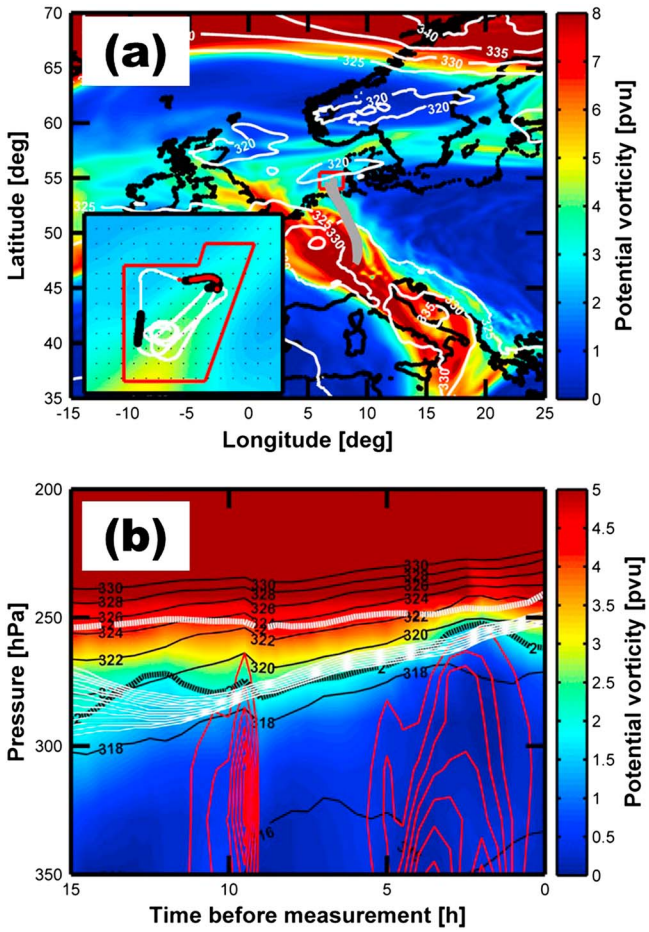

Figure 4. (a) Potential vorticity (PV) (color) and potential temperature Θ (white contour lines) at 250 hPa from ECMWF data (15 UTC). Gray lines show 15 h backward trajectories filtered for backward trajectories with PV ($t = 0$ h) > 3 pvu along the flight path and PV values lower than 1.5 pvu before. The red box is enlarged in the bottom left corner with the restricted flight area (red line), flight path (white line), location of observed stratospheric cirrus particles (red dots), and starting points for filtered backward trajectories (black dots). (b) Vertical cross section of PV (color) and Θ (black contour lines) along the backward trajectories (white lines) starting at the observation of the stratospheric cirrus particles. The thick black line highlights the 2 pvu isoline, and the thick white line is the thermal tropopause according to *WMO* [1957]. Cloud occurrence (ice water content, no units) in ECMWF data is marked with red contour lines.

5. Formation and Transport of the Detected Cirrus Particles

The origin of the stratospheric air masses containing the cirrus particles is investigated by 15 h backward trajectories using the Lagrangian Analysis Tool (LAGRANTO) as described by *Wernli and Davies* [1997]. The trajectories were driven by horizontal and vertical winds from operational analysis data (T1279L91) provided by the European Centre for Medium-Range Weather Forecast (ECMWF) interpolated onto a regular grid of 0.125° horizontal spacing. The trajectories were initialized along the flight path (every 1 s). The PV distribution (Figure 4a) illustrates that the measurements were affected by a stratospheric filament as indicated by the horizontal PV gradient at 250 hPa corresponding to the flight level. It also shows that the region of measured cirrus occurrence partly coincides with the location of trajectories indicating troposphere-to-stratosphere transport. The vertical cross section along the backward trajectories (Figure 4b) shows a slow ascent in the last 15 h before the measurement and transport of the probed air masses across the 2 pvu isoline at the top of a cloud layer in the last 3 h before detecting the ice crystals. Relative humidity over ice (RH_e) (not shown) along the trajectories is continuously rising from $RH_e < 70\%$ ($t = -15$ h) to $RH_e \approx 110\%$ ($t = -2$ h). Increasing PV values between $t = -2$ h and $t = 0$ h are accompanied by decreasing RH_e from 110% to approximately 100%. It is concluded that during the lifting of humid, tropospheric air masses, a cirrus cloud forms close to the tropopause. Subsequent diabatic processes at the top of this cirrus cloud, as described in *Fusina and Spichtinger* [2010] and *Fusina et al.* [2007], might be a plausible mechanism for

triggering turbulence and mixing of tropospheric and stratospheric air masses in this case. Other processes like rapid frontal uplift or convection can be excluded from meteorological analysis. The extension of the backward trajectories to $t = -5$ days indicates no significant stratospheric influence. Therefore, the measurement of the stratospheric ice particles due to a mixing event with $t < -15$ h is very unlikely. Further investigation of the detailed exchange mechanism would require a detailed model analysis, which is beyond the scope of this paper.

6. Summary

Based on in situ measurements during AIRTOSS-ICE 2013, cirrus particles in an air mass influenced by the stratosphere were identified. From high-precision N_2O measurements by the newly developed UMAQS instrument an N_2O threshold, which is indicative for stratospheric air, was determined. The CO-N_2O mixing diagram shows that the air mass with the cirrus particles consists of a mixture of tropospheric and stratospheric air. From backward trajectories it is concluded that these cirrus particles were formed during slow ascent in the troposphere and subsequently transported across the dynamical tropopause.

To our best knowledge, this is the first direct in situ observation of irreversible mixing of tropospheric with stratospheric air associated with cirrus cloud occurrence in the extratropical tropopause region. From the analysis of the large-scale dynamics and local meteorological data it is concluded that small-scale processes are of major importance in this case study. Nevertheless, an unambiguous verification of the exchange triggering process cannot be given, even if the impact of radiative forcing at the top of cirrus clouds can modify the local thermal tropopause and might be the key parameter in this case. This corroborates the conclusions of *Riese et al.* [2012], highlighting the importance of the detailed understanding of stratosphere-troposphere exchange (STE) at the tropopause for a correct quantification of the radiation budget.

Besides this issue the capability of fast and precise N_2O measurements as a marker for STE superior to other trace gases could be demonstrated. These measurements are capable of investigating exchange processes in the tropopause region in more detail.

Acknowledgments

We thank two anonymous reviewers for their very helpful and constructive comments. Furthermore, we acknowledge the Aeronautical Meteorology Department of the Deutscher Wetterdienst, Offenbach, for providing satellite images during the flight campaign. We particularly thank enviscope GmbH and the Gesellschaft für Flugzieldarstellung mbH (GFD) for the execution of the flights and their excellent support during the campaign. We also would like to thank Aerodyne Research Inc., MA, USA, and the electronics department of the MPIC Mainz for their assistance in preparation of the first airborne deployment of UMAQS. Main funding for the AIRTOSS-ICE project was provided by the German Science Foundation (DFG) through the "Spatially Inhomogeneous Cirrus: Influence on Atmospheric Radiation" project (BO1829/7-1) with additional significant support from internal resources of the Max Planck Society. Further information on the data relevant to this paper can be obtained upon request via email to the author (stefan.mueller@uni-mainz.de).

The Editor thanks two anonymous reviewers for their assistance in evaluating this paper.

References

Assonov, S., C. Brenninkmeijer, T. Schuck, and T. Umezawa (2013), N_2O as a tracer of mixing stratospheric and tropospheric air based on CARIBIC data with applications for CO_2, *Atmos. Environ.*, *79*, 769–779, doi:10.1016/j.atmosenv.2013.07.035.

Bethan, S., G. Vaughan, and S. J. Reid (1996), A comparison of ozone and thermal tropopause heights and the impact of tropopause definition on quantifying the ozone content of the troposphere, *Q. J. R. Meteorol. Soc.*, *122*(532), 929–944, doi:10.1002/qj.49712253207.

Birner, T. (2006), Fine-scale structure of the extratropical tropopause region, *J. Geophys. Res.*, *111*, D04104, doi:10.1029/2005JD006301.

Birner, T., A. Dörnbrack, and U. Schumann (2002), How sharp is the tropopause at midlatitudes?, *Geophys. Res. Lett.*, *29*(14), 1700, doi:10.1029/2002GL015142.

Borrmann, S., S. Solomon, J. E. Dye, and B. Luo (1996), The potential of cirrus clouds for heterogeneous chlorine activation, *Geophys. Res. Lett.*, *23*(16), 2133–2136, doi:10.1029/96GL01957.

de Reus, M., et al. (2009), Evidence for ice particles in the tropical stratosphere from in-situ measurements, *Atmos. Chem. Phys.*, *9*(18), 6775–6792, doi:10.5194/acp-9-6775-2009.

Dye, J. E., and D. Baumgardner (1984), Evaluation of the forward scattering spectrometer probe. Part I: Electronic and optical studies, *J. Atmos. Ocean. Technol.*, *1*(4), 329–344, doi:10.1175/1520-0426(1984)001<0329:EOTFSS>2.0.CO;2.

Fahey, D. W., et al. (1995), Emission measurements of the concorde supersonic aircraft in the lower stratosphere, *Science*, *270*(5233), 70–74, doi:10.1126/science.270.5233.70.

Fischer, H., F. G. Wienhold, P. Hoor, O. Bujok, C. Schiller, P. Siegmund, M. Ambaum, H. A. Scheeren, and J. Lelieveld (2000), Tracer correlations in the northern high latitude lowermost stratosphere: Influence of cross-tropopause mass exchange, *Geophys. Res. Lett.*, *27*(1), 97–100, doi:10.1029/1999GL010879.

Frey, W., H. Eichler, M. de Reus, R. Maser, M. Wendisch, and S. Borrmann (2009), A new airborne tandem platform for collocated measurements of microphysical cloud and radiation properties, *Atmos. Meas. Tech.*, *2*(1), 147–158, doi:10.5194/amt-2-147-2009.

Frey, W., et al. (2011), In situ measurements of tropical cloud properties in the West African Monsoon: Upper tropospheric ice clouds, Mesoscale Convective System outflow, and subvisual cirrus, *Atmos. Chem. Phys.*, *11*(12), 5569–5590, doi:10.5194/acp-11-5569-2011.

Fusina, F., and P. Spichtinger (2010), Cirrus clouds triggered by radiation, a multiscale phenomenon, *Atmos. Chem. Phys.*, *10*(11), 5179–5190, doi:10.5194/acp-10-5179-2010.

Fusina, F., P. Spichtinger, and U. Lohmann (2007), Impact of ice supersaturated regions and thin cirrus on radiation in the midlatitudes, *J. Geophys. Res.*, *112*, D24S14, doi:10.1029/2007JD008449.

Gettelman, A., P. Hoor, L. L. Pan, W. J. Randel, M. I. Hegglin, and T. Birner (2011), The extratropical upper troposphere and lower stratosphere, *Rev. Geophys.*, *49*, RG3003, doi:10.1029/2011RG000355.

Gurk, C., H. Fischer, P. Hoor, M. G. Lawrence, J. Lelieveld, and H. Wernli (2008), Airborne in-situ measurements of vertical, seasonal and latitudinal distributions of carbon dioxide over Europe, *Atmos. Chem. Phys.*, *8*(21), 6395–6403, doi:10.5194/acp-8-6395-2008.

Hoor, P., H. Fischer, L. Lange, J. Lelieveld, and D. Brunner (2002), Seasonal variations of a mixing layer in the lowermost stratosphere as identified by the CO-O_3 correlation from in situ measurements, *J. Geophys. Res.*, *107*(D5), 4044, doi:10.1029/2000JD000289.

Hoskins, B. J., M. E. McIntyre, and A. W. Robertson (1985), On the use and significance of isentropic potential vorticity maps, *Q. J. R. Meteorol. Soc.*, *111*(470), 877–946, doi:10.1002/qj.49711147002.

Jiang, X., W. L. Ku, R.-L. Shia, Q. Li, J. W. Elkins, R. G. Prinn, and Y. L. Yung (2007), Seasonal cycle of N_2O: Analysis of data, *Global Biogeochem. Cycles*, *21*, GB1006, doi:10.1029/2006GB002691.

Keckhut, P., A. Hauchecorne, S. Bekki, A. Colette, C. David, and J. Jumelet (2005), Indications of thin cirrus clouds in the stratosphere at mid-latitudes, *Atmos. Chem. Phys.*, *5*(12), 3407–3414, doi:10.5194/acp-5-3407-2005.

Kort, E. A., P. K. Patra, K. Ishijima, B. C. Daube, R. Jiménez, J. Elkins, D. Hurst, F. L. Moore, C. Sweeney, and S. C. Wofsy (2011), Tropospheric distribution and variability of N_2O: Evidence for strong tropical emissions, *Geophys. Res. Lett.*, *38*, L15806, doi:10.1029/2011GL047612.

Kunz, A., P. Konopka, R. Müller, and L. L. Pan (2011), Dynamical tropopause based on isentropic potential vorticity gradients, *J. Geophys. Res.*, *116*, D01110, doi:10.1029/2010JD014343.

Logan, J. A. (1999), An analysis of ozonesonde data for the troposphere: Recommendations for testing 3-D models and development of a gridded climatology for tropospheric ozone, *J. Geophys. Res.*, *104*(D13), 16,115–16,149, doi:10.1029/1998JD100096.

McManus, J. B., D. D. Nelson, and M. S. Zahniser (2010), Long-term continuous sampling of $^{12}CO_2$, $^{13}CO_2$ and $^{12}C^{18}O^{16}O$ in ambient air with a quantum cascade laser spectrometer, *Isot. Environ. Health Stud.*, *46*(1), 49–63, doi:10.1080/10256011003661326.

McManus, J. B., M. S. Zahniser, and D. D. Nelson (2011), Dual quantum cascade laser trace gas instrument with astigmatic Herriott cell at high pass number, *Appl. Opt.*, *50*(4), A74–A85, doi:10.1364/AO.50.000A74.

Montoux, N., P. Keckhut, A. Hauchecorne, J. Jumelet, H. Brogniez, and C. David (2010), Isentropic modeling of a cirrus cloud event observed in the midlatitude upper troposphere and lower stratosphere, *J. Geophys. Res.*, *115*, D02202, doi:10.1029/2009JD011981.

Pan, L. L. (2004), Definitions and sharpness of the extratropical tropopause: A trace gas perspective, *J. Geophys. Res.*, *109*, D23103, doi:10.1029/2004JD004982.

Randel, W. J., D. J. Seidel, and L. L. Pan (2007), Observational characteristics of double tropopauses, *J. Geophys. Res.*, *112*, D07309, doi:10.1029/2006JD007904.

Riese, M., F. Ploeger, A. Rap, B. Vogel, P. Konopka, M. Dameris, and P. Forster (2012), Impact of uncertainties in atmospheric mixing on simulated UTLS composition and related radiative effects, *J. Geophys. Res.*, *117*, D16305, doi:10.1029/2012JD017751.

Solomon, S., S. Borrmann, R. R. Garcia, R. Portmann, L. Thomason, L. R. Poole, D. Winker, and M. P. McCormick (1997), Heterogeneous chlorine chemistry in the tropopause region, *J. Geophys. Res.*, *102*(D17), 21,411–21,429, doi:10.1029/97JD01525.

Spang, R., G. Günther, M. Riese, L. Hoffmann, R. Müller, and S. Griessbach (2014), Satellite observations of cirrus clouds in the Northern Hemisphere lowermost stratosphere, *Atmos. Chem. Phys. Discuss.*, *14*(8), 12,323–12,375, doi:10.5194/acpd-14-12323-2014.

Stratospheric Processes and their Role in Climate (2013), SPARC report on the lifetimes of stratospheric ozone-depleting substances, their replacements, and related species, *SPARC Rep. No. 6, WCRP-15/2013*, World Meteorol. Organ., World Climate Res. Programme. [Available at http://www.sparc-climate.org/publications/sparc-reports/sparc-report-no6/, Last access 4 February 2015.]

Spichtinger, P., K. Gierens, U. Leiterer, and H. Dier (2003a), Ice supersaturation in the tropopause region over Lindenberg, Germany, *Meteorol. Zeitschrift*, *12*(3), 143–156, doi:10.1127/0941-2948/2003/0012-0143.

Spichtinger, P., K. Gierens, and W. Read (2003b), The global distribution of ice-supersaturated regions as seen by the Microwave Limb Sounder, *Q. J. R. Meteorol. Soc.*, *129*(595), 3391–3410, doi:10.1256/qj.02.141.

Wendisch, M., and J. L. Brenguier (Eds.) (2013), *Airborne Measurements for Environmental Research: Methods and Instruments*, 655 pp., Wiley-VCH Verlag GmbH and Co. KGaA, Weinheim, Germany, doi:10.1002/9783527653218.

Wernli, B. H., and H. C. Davies (1997), A Lagrangian-based analysis of extratropical cyclones. I: The method and some applications, *Q. J. R. Meteorol. Soc.*, *123*(538), 467–489, doi:10.1002/qj.49712353811.

Wirth, V. (2003), Static stability in the extratropical tropopause region, *J. Atmos. Sci.*, *60*(11), 1395–1409, doi:10.1175/1520-0469(2003)060<1395:SSITET>2.0.CO;2.

World Meteorological Organization (WMO) (1957), Meteorology: A three-dimensional science, *WMO Bull.*, *6*, 134–138.

Zahn, A., et al. (2000), Identification of extratropical two-way troposphere-stratosphere mixing based on CARIBIC measurements of O_3, CO, and ultrafine particles, *J. Geophys. Res.*, *105*(D1), 1527–1535, doi:10.1029/1999JD900759.